# Measurement of the Rb($5D_{5/2}$) photoionization cross section using trapped atoms

B. C. Duncan, V. Sanchez-Villicana,* and P. L. Gould
*Department of Physics, U-3046, University of Connecticut, Storrs, Connecticut 06269-3046*

H. R. Sadeghpour
*Institute for Theoretical Atomic and Molecular Physics, Harvard-Smithsonian Center for Astrophysics, 60 Garden Street, Cambridge, Massachusetts 02138*

(Received 4 August 2000; published 15 March 2001)

We report on measurements of the cross section for photoionization of Rb atoms in the highly excited $5D_{5/2}$ level at wavelengths ranging from 1064 to 532 nm (photoelectron energies of 0.175 to 1.34 eV). We efficiently populate the $5D_{5/2}$ level using coherent two-photon excitation of trapped atoms with pulses in the counter-intuitive order. The absolute photoionization cross sections are then measured via the increased loss of atoms from the magneto-optical trap when it is illuminated by the photoionizing light. Our results are in good agreement with new calculations based on the valence-electron parametric potential method.

DOI: 10.1103/PhysRevA.63.043411 PACS number(s): 32.80.Pj, 32.80.Fb

## I. INTRODUCTION

The techniques of laser cooling and trapping [1] have enabled many new directions in atomic and molecular physics, including metrology, quantum collective effects, ultracold collisions, and photoassociative spectroscopy. One benefit of long trapping times is that any process which causes the ejection of atoms from the trap can be measured by the corresponding trap loss rate. Photoionization is one such process [2]. When ionizing light is incident on a sample of trapped atoms, atoms are lost as they are ionized. The measured loss rate per atom, combined with the ionizing intensity and fraction of time spent in the relevant atomic state, yields the absolute photoionization cross section. This technique does not require knowledge of the atomic density and furthermore, since ions are not actually detected, problems with ion detector calibration are avoided. Since the initial demonstration of this technique with photoionization of the $5P_{3/2}$ level of Rb [2], it has been fruitfully applied in other experiments involving Rb [3], Cs [4,5], and Mg [6,7]. A variation of this trap loss technique has also been used to measure the absolute cross sections for electron collisional processes [8,9].

Excited-state photoionization (PI) is an important process in many areas of atomic physics. Examples include plasma discharges, laser-guided plasmas, laser gain media, and sensitive and state-selective atomic detection. Radiative recombination, the inverse of PI, is important in low temperature (e.g., astrophysical) plasmas, so PI is relevant in this context as well. Since PI depends sensitively on nonhydrogenic atomic wave functions, measurements of absolute PI cross sections and their energy dependence provide useful tests of atomic theory.

PI from the first excited $P$ states in alkali-metal atoms has received considerable theoretical and experimental attention [10,11]. Excited D states have also been investigated in various systems [12–15], stimulated in part by predictions of multiple minima in the cross sections [16]. In the present work, we use the trap loss technique to measure the absolute PI cross section from the Rb($5D_{5/2}$) level at various wavelengths for the first time. Agreement with new theoretical calculations, presented here, is good. This work also represents the first time that the trap loss technique [2] has been extended to highly excited states, i.e., states not populated by the trapping laser. PI of the high-lying $5D_{5/2}$ level, which is bound by 0.99 eV, is of particular interest because this process is energetically allowed during two-photon excitation from the $5S_{1/2}$ ground state. Therefore, this loss mechanism must be understood in any experiment (e.g., ultracold collisions) involving excitation of trapped atoms to the $5D$ level.

The paper is organized as follows. In Sec. II, we describe the experiment. In Sec. III, we present the measurements of the PI cross Section. The cross section calculations and the comparison with experiment are described in Sec. IV. Section V is a summary.

## II. EXPERIMENT

The basic idea of the experiment is to excite a trapped sample of Rb to the $5D_{5/2}$ level and then expose these atoms to photoionizing light and measure their loss rate from the trap. The photoionization (PI) measurements employ either continuous (cw) or pulsed lasers, depending on the wavelength. In the case of cw PI, the trapped atoms are repetitively excited with laser pulses to the $5D_{5/2}$ level, resulting in a time-averaged excited-state fraction $f_{5D}$. A trapped atom is ionized at an average rate which is proportional to the product of $f_{5D}$ and the PI laser intensity $I_{\mathrm{PI}}$. In the case of pulsed PI, the probability of ionization by a single PI pulse is measured by the instantaneous loss of atoms following that pulse. In the following paragraphs, we briefly describe the important aspects of the experiment: the magneto-optical trap, the $5D_{5/2}$ excitation process, and the photoionization.

The experiment is performed on a low temperature ($\sim 500\ \mu$K) ensemble of $^{85}$Rb atoms captured from room-temperature vapor [17] into a diode-laser based magneto-optical trap (MOT). The trap laser is detuned about 10 MHz

*Permanent address: Instituto Nacional de Astrofisica, Optica y Electronica, Tonanzintla, Puebla 72840, Mexico.

 

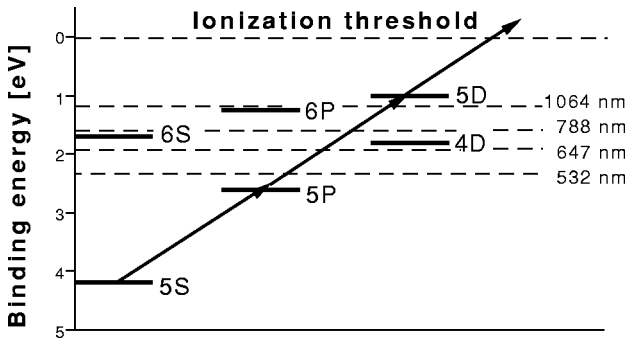


FIG. 1. Energy levels of the Rb atom which are relevant to the 5D photoionization (PI) measurements. Fine and hyperfine structure are not shown. The 5D level is populated by two-photon STIRAP excitation through the $5P$ level and subsequently photoionized by either pulsed or cw laser light. The dashed lines mark the binding energies which can be ionized by light of the indicated wavelength.

below the $D_2$ cycling transition at 780 nm $[5S_{1/2}(F=3) \rightarrow 5P_{3/2}(F'=4)]$ and a repumping laser, tuned near the $D_1$ transition at 795 nm $[5S_{1/2}(F=2) \rightarrow 5P_{1/2}(F'=3)]$, prevents population from accumulating in the $F=2$ level. Both lasers are Littrow-configuration linewidth-narrowed diode lasers [18] electronically locked to saturated absorption features. The trap and repump lasers pass through independent acousto-optic modulators (AOMs) in order that they may be turned off when the $5D_{5/2}$ excitation is performed. The cycle time is typically 20 $\mu$s, with the trap and repump on together for 17 $\mu$s and a 3 $\mu$s window for $5D_{5/2}$ excitation. The total trap laser intensity (sum of all six beams) is typically 12 mW/cm$^2$ and the beam diameters are $\sim$ 5 by 4 mm full-width at half-maximum (FWHM). Two coils in an ''anti-Helmholtz'' arrangement produce an axial magnetic field gradient of approximately 22 G/cm. Typically the trapped cloud is $\sim$120 $\mu$m in $1/e$ radius and contains about $5 \times 10^5$ atoms. The loading time, in the absence of $5D_{5/2}$ excitation or photoionization, is $\sim$1.5 s.

The sample of cold atoms is efficiently excited to the $5D_{5/2}$ level by a pulsed two-photon transition: $5S_{1/2} \rightarrow 5P_{3/2} \rightarrow 5D_{5/2}$ (see Fig. 1) with pulses in the counterintuitive order [19], i.e., the upper transition is driven first. This is a variation of stimulated Raman adiabatic passage (STIRAP) [20] and is described in detail in [19]. The pulses are supplied by two high-power (100 mW) slave diode lasers which are individually injection-locked by linewidth-narrowed ($\leqslant$1.5 MHz) master diode lasers. The $5S \rightarrow 5P$ master laser is locked near the $5S_{1/2}(F=3) \rightarrow 5P_{3/2}(F'=4)$ transition at 780 nm using saturated absorption in a magnetic field [21]. This diode also provides the first step in Doppler-free two-color two-photon spectroscopy [22] in a room-temperature cell which is used to lock the $5P \rightarrow 5D$ master laser near the $5P_{3/2}(F'=4) \rightarrow 5D_{5/2}(F''=5)$ transition at 776 nm. The light incident on the trapped sample is two-photon resonant with an intermediate state detuning $\Delta/2\pi = +47$ MHz. Both slave lasers are controlled with AOM's, creating near-Gaussian pulses of $\sim$30 ns (FWHM) duration and $\sim$15 ns separation, with the $5P \rightarrow 5D$ pulse arriving before the $5S \rightarrow 5P$ pulse (counterintuitive order). The counterpropagating STIRAP pulses illuminate the cold atoms during the 3 $\mu$s window when the trap and repump AOM's are turned off. Their intensity profiles are near-Gaussian with average sizes about 450 $\mu$m in $1/e$ radius. Peak intensities are 4 W/cm$^2$. We monitor the $5D_{5/2}$ excitation by detecting, with a photomultiplier and filter, the 420 nm fluorescence emitted in the second step of the $5D \rightarrow 6P \rightarrow 5S$ decay path. The resonance fluorescence at 780 nm is also selectively detected and used as a measure of the relative number of trapped atoms.

We use three sources of light for photoionization (PI). Continuous (cw) light at 647 and 788 nm are provided by a krypton-ion laser and a free-running diode laser, respectively. A Nd:YAG pulsed laser, externally triggered at 1 Hz, provides the 1064 nm (fundamental) and 532 nm (second harmonic) wavelengths. The beam sizes ($1/e$ radii) are typically 1.25 mm for the 1064 nm, 750 $\mu$m for the 532 nm, 450 $\mu$m for the 647 nm, and 380 $\mu$m for the 788 nm. The smaller size of the trapped cloud ensures that the atoms experience a spatially uniform intensity. For the cw light, the peak intensity is determined by measuring the total power and the two-dimensional laser beam profile. Similarly, for the pulsed light, the peak fluence is determined by measuring the pulse energy and the beam profile.

## III. MEASUREMENTS

We first discuss the measurement technique for cw PI. Each STIRAP pulse pair transfers a fraction $\eta$ of the trapped sample to the $5D_{5/2}$ level, from which radiative decay occurs with a lifetime $\tau = 241$ ns [23]. PI occurs at a rate $\Phi\sigma$ while in the $5D_{5/2}$ level, where $\Phi = I\lambda/hc$ is the PI photon flux, $\sigma$ the PI cross section, I the intensity, $\lambda$ the wavelength, $c$ the speed of light, and $h$ Planck's constant. Accounting for complete exponential decay of the $5D_{5/2}$ level, the PI probability per STIRAP pulse pair is $\Phi\sigma\eta\tau$. If STIRAP is repeated at a rate $R_{\rm rep}$, the time-averaged PI rate is given by $\langle\Gamma_{\rm PI}\rangle = \Phi\sigma\eta\tau R_{\rm rep} = \Phi\sigma f_{\rm 5D}$ where $f_{\rm 5D} = \eta\tau R_{\rm rep}$ is the time-averaged excited-state fraction (typically $<1\%$).

The time evolution of the number of atoms $N$ in a vapor-cell MOT is described by

$$\dot{N} = L - \Gamma_0 N - \langle\Gamma_{PI}\rangle N, \tag{1}$$

where L is the loading rate (atoms/s) and $\Gamma_0$ is the total loss rate (per atom) of atoms from the MOT in the absence of PI. We note that $\Gamma_0$ includes collisions of trapped atoms with background gas, ultracold inelastic collisions between trapped atoms, and loss induced by the $5D_{5/2}$ excitation. The loss rate due to ultracold collisions is constant in the regime of constant density [24], i.e., when N is sufficiently large that the density is limited by radiation trapping. The steady-state solution to Eq. (1) is

$$N_0 = L/(\Gamma_0 + \langle\Gamma_{\rm PI}\rangle) \tag{2}$$

and the approach to steady state, starting with an empty trap, is exponential [3]. The total loss rate $\Gamma_0 + \langle\Gamma_{PI}\rangle$ is the inverse of the measured loading time constant. In Fig. 2, we show an example of the effect of PI on the number of trapped

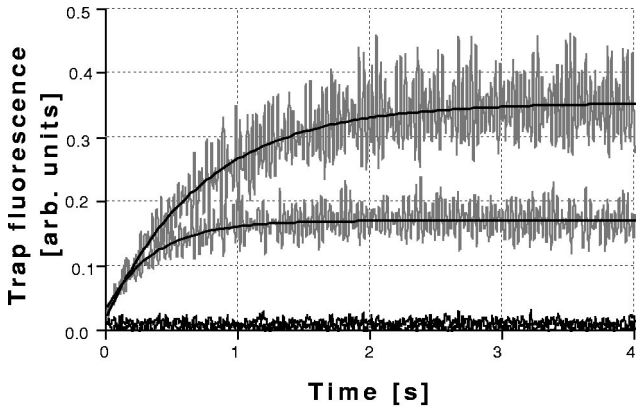


FIG. 2. An example of the effect of cw photoionizing light (6.9 W/cm$^2$ at 788 nm) on the number of trapped atoms, as measured by their fluorescence. The trap is turned on at $t=0$. In the upper trace, only the STIRAP excitation is present, while in the lower trace, both STIRAP excitation and photoionization are present, resulting in a more rapid loading of the trap and a smaller steady-state number of trapped atoms. The dashed lines are fits to exponential loading curves. The bottom two curves are zero levels recording all stray light with the trapping magnetic field off.

atoms (as measured by their fluorescence). Loading transients are seen when the MOT is turned on and the steady-state number is seen to decrease in the presence of PI. To eliminate scattered light contributions and background atom fluorescence, zero levels are determined by turning off only the MOT magnetic field coils. For these cw measurements the PI light is on continuously, and we have verified that, in the absence of $5D_{5/2}$ excitation, it has no observable effect on the MOT.

In Fig. 3, the dependence of $N_0$ on PI intensity I is displayed, along with a fit to Eq. (2). From this fit and the measured value of $\Gamma_0$, we obtain the PI cross section $\sigma$. The value of $\eta$ is determined by pulsed PI as discussed below. In Fig. 4, the total loss rate $\Gamma_0+\langle\Gamma_{\mathrm{PI}}\rangle$, as derived from the loading transients, is plotted as a function of PI intensity. A linear fit yields another determination of $\sigma$. Values obtained

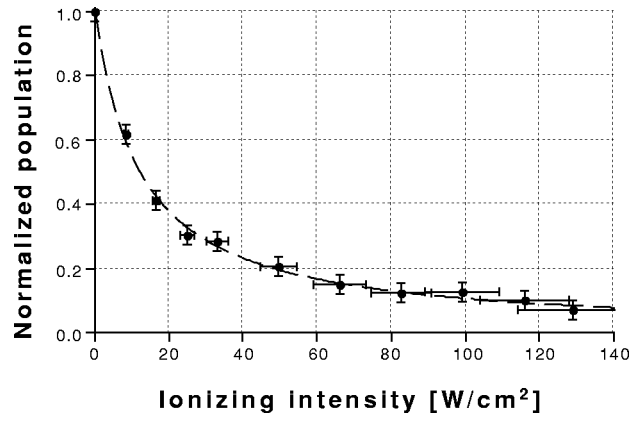


FIG. 3. Plot of the fractional steady-state number of trapped atoms as a function of cw photoionizing intensity at 788 nm. The dashed line is a fit to Eq. (2), which allows the PI cross section to be extracted.

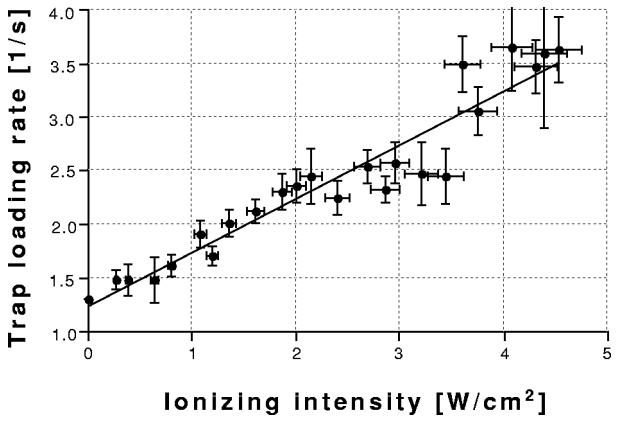


FIG. 4. Plot of the total trap loss rate, determined from loading curves, as a function of photoionizing intensity at 788 nm. The solid line is a linear fit from which $\Gamma_0$ and the PI cross section are determined.

from these loading curves are less accurate than, but consistent with, values obtained from the steady-state number of atoms in the trap. They are not used in the final cross section determinations.

For cw PI, there are several potential complications to the simple model [Eq. (1)]. First, if the PI intensity is high enough to cause significant ionization during the $5D_{5/2}$ lifetime, the PI loss will saturate. However, our highest cw intensities fall short of saturation by three orders of magnitude. Second, at large values of $I$, the loading rate $L$ can be reduced by ionization of atoms as they enter the trap [3,4]. In our case, however, the relevant ($5D_{5/2}$) excitation is produced by focused beams which occupy a very small fraction of the capture volume of the MOT, thereby minimizing any effect on the loading. Third, at small $N_0$ (large $I$), the density may begin to decrease from its radiation-trapping-limited value, which would reduce the loss rate due to ultracold collisions. However, this loss rate is a small fraction of the PI-induced loss rate at the high intensities where this effect would occur. Finally, the ions and photoelectrons could recombine back into neutral atoms and be recaptured by the trap [25]. This would act as a source term in Eq. (1) and reduce the apparent loss rate of atoms at high intensities. Such a recombination effect should be strongly enhanced at low photoelectron energies. Under our conditions, we see no evidence for any of these potential complicating effects.

For pulsed PI, a different technique for extracting the cross section is used. Light from a pulsed Nd:YAG laser (fundamental at 1064 nm or second harmonic at 532 nm) is synchronized to arrive immediately following the $5D_{5/2}$ excitation. The short duration of the PI pulse (5–7 ns FWHM) relative to the radiative lifetime of the $5D_{5/2}$ level (241 ns [23]) ensures that the initial $5D_{5/2}$ population is sampled before it has a chance to decay. The ionizing fluence $F=\int_{-\infty}^{\infty} I dt$ can be sufficiently high to ionize a significant fraction of the $5D_{5/2}$ population in a single pulse. An example is shown in Fig. 5, where the number of trapped atoms is seen to drop sharply following a single PI pulse. The trap subsequently reloads towards its steady-state value. A fit to an exponential loading curve, also shown in Fig. 5, serves to

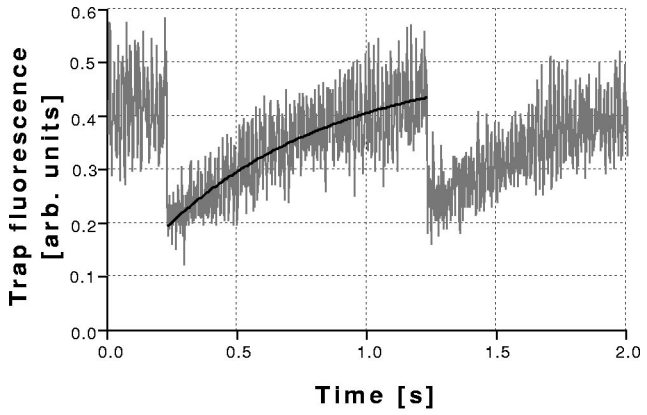


FIG. 5. Instantaneous trap loss induced by pulsed photoionization at 1064 nm. The PI laser fires once per second, coincident with the STIRAP excitation, and ionizes a significant fraction of atoms in the trap. This results in a sudden drop in the trap fluorescence, followed by reloading of the trap.

establish the minimum trapped atom fluorescence signal and therefore the fraction of atoms which are ionized.

An atom in the $5D_{5/2}$ level is ionized at a rate $I\sigma\lambda/hc$, so in a single short pulse, the probability of a trapped atom being lost due to ionization is given by

$$P_{PI}=\eta(1-e^{-\sigma F\lambda/hc}), \tag{3}$$

where $\eta$ is the excitation efficiency to the $5D_{5/2}$ level. In the limit of saturated ionization, $P_{\mathrm{PI}}$ is a direct measure of $\eta$ (typically $\sim$50%), while in the unsaturated regime, the variation of $P_{\mathrm{PI}}$ with $F$ gives the PI cross section. A plot of $P_{\mathrm{PI}}$ vs. $F$, along with a fit to Eq. (3), is shown in Fig. 6. Since the values of $\eta$ obtained from this pulsed PI data are very direct, they are used in extracting the cw PI cross sections as well.

The cw measurements assume that the $5D_{5/2}$ population decays radiatively with a lifetime of 241 ns. It is important to check this assumption because of the possibility of collective radiation (e.g., on the $5D_{5/2}\rightarrow 6P_{3/2}$ transition at 5.2 $\mu$m) in the cold dense sample which could effectively shorten the

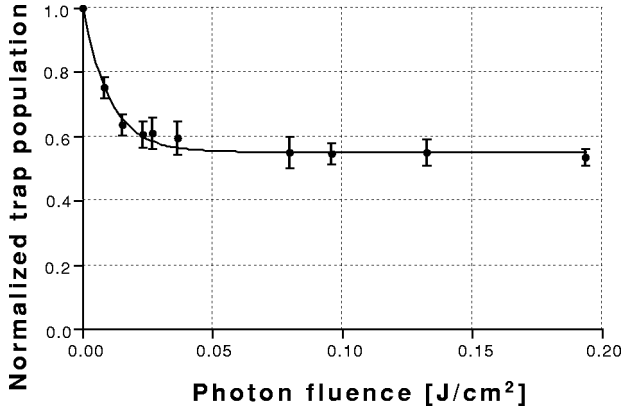


FIG. 6. Plot of fraction of atoms remaining in the trap following a PI pulse (1064 nm) as a function of photon fluence. Saturation to a nonzero value is a result of incomplete STIRAP excitation. The solid line is a fit to $1-P_{\mathrm{PI}}$ where $P_{\mathrm{PI}}$ is given by Eq. (3).

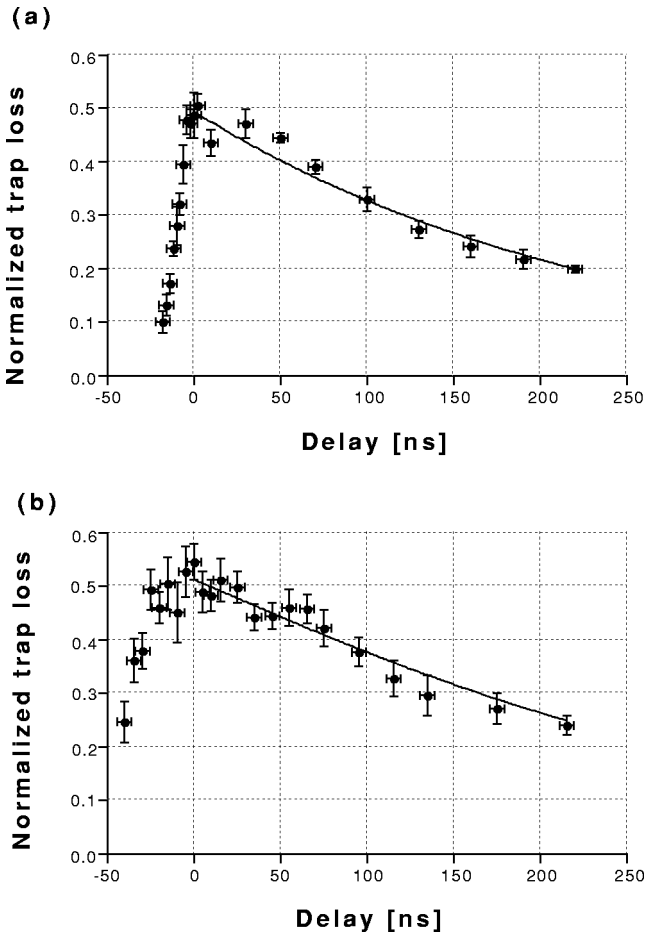


FIG. 7. (a) Fraction of atoms lost from the trap as a function of delay between the STIRAP excitation and the PI pulse (1064 nm). The exponential decay, fit with the solid line, reflects the radiative decay of the 5D population. The fits yields a lifetime of 245(16) ns. (b) Same as (a), but at 532 nm. The fit includes PI loss from the 6P level which is populated by radiative cascade. The known lifetimes and calculated PI cross sections are fixed in the fit.

lifetime. Since light at 1064 nm can only photoionize the $5D_{5/2}$ level (the $6P_{3/2}$ level requires $\lambda<1010$ nm for PI), pulsed PI at this wavelength allows us to directly measure the decay. The fractional ionization of the trap is proportional to the instantaneous $5D_{5/2}$ population, so delaying the PI pulse relative to the $5D_{5/2}$ excitation maps out the $5D_{5/2}$ decay. An example is shown in Fig. 7(a), along with a fit to an exponential decay which yields, within error, the expected lifetime of 241 ns [23].

On the other hand, light at 532 nm is energetically capable of photoionizing the $6P_{3/2}$ level. Therefore the dependence of ionization fraction on delay should reflect the temporal evolution of both the $5D_{5/2}$ and $6P_{3/2}$ levels, weighted by their respective PI cross sections. Lower states ($6S_{1/2}$,$4D_{5/2}$,$4D_{3/2}$) can also be photoionized, but contribute negligibly to this decay curve. The $5D_{5/2}$ population decays exponentially ($\tau_{5D}=241$ ns) after the excitation with a branching ratio of 0.35 to $6P_{3/2}$. This feeding of the $6P_{3/2}$ level, coupled with its decay ($\tau_{6P}=109$ ns [23]), yields a maximum $6P_{3/2}$ population of 12% of the initial $5D_{5/2}$ popu-

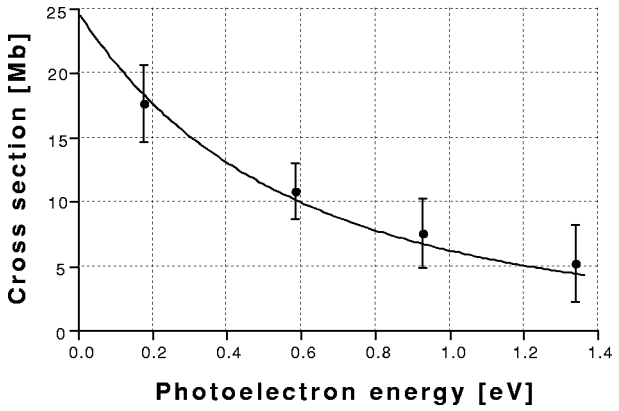


FIG. 8. Plot of the $5D_{5/2}$ PI cross section as a function of photon energy above threshold (photoelectron energy). The data points correspond to wavelengths (left to right) of 1064, 788, 647, and 532 nm. The solid line is the theoretical prediction.

lation at a delay of $\tau_{6P}$. The fractional ionization measurement is shown in Fig. 7(b), along with a fit to the expected time dependence, assuming the theoretically calculated PI cross sections. The relatively large error bars, due to shot-to-shot fluctuations in fluence, do not allow the relative cross sections to be extracted. However, the data are consistent with the predicted temporal dependence.

The cross section results are summarized in Fig. 8, where they are plotted as a function of the energy (above threshold) of the photoionizing light. The uncertainties are dominated by the statistics of cross section determinations from a number (typically 5) of experimental runs. For the points using cw PI light ($\lambda = 647$ and 788 nm), we have included a correction to account for PI from the $6P_{3/2}$ level, which is populated by cascade from $5D_{5/2}$, and from which PI is energetically allowed. The combination of the 35% branching ratio for $5D_{5/2} \rightarrow 6P_{3/2}$ and the 109 ns $6P_{3/2}$ lifetime results in an initially excited $5D_{5/2}$ atom spending, on average, 16% as much time in $6P_{3/2}$ as in $5D_{5/2}$. The measured PI cross section includes the appropriately weighted contribution from $6P_{3/2}$. This contribution, based on a calculated $6P_{3/2}$ PI cross section ($\sigma = 8.5$, 6.6, and 4.8 Mb at $\lambda = 788$, 647, and 532 nm, respectively), has been subtracted in the data shown in Fig. 8. These cross section calculations are similar to those described in Sec. IV, but with a uniform $m_F$ distribution. This correction lowers the cross section from 12.2 to 10.9 Mb for 788 nm and from 8.6 to 7.6 Mb for 647 nm. We note that the $6S_{1/2}, 4D_{5/2}$, and $4D_{3/2}$ levels can contribute in a similar manner, i.e., they can be ionized by 647 nm light. However, based on the branching ratios to these levels and their lifetimes [23], these contributions should be negligible. Compared to the average time (241 ns) spent in the $5D_{5/2}$ level, a cascading atom will spend 3.7%, 2.2.%, and 0.2% as much time in the $6S_{1/2}, 4D_{5/2}$, and $4D_{3/2}$ levels, respectively. The photoionization trap loss measurements have been carried out with the two counterpropagating STIRAP beams linearly polarized at a relative angle of typically 30°. Changing this angle from 0° to 90°, we did not observe a statistically significant difference ($<10\%$) in the PI-induced trap loss. Similarly, we have varied the polarization of the photoionizing light and not seen a statistically significant difference ($<15\%$) in the fractional trap loss when it is perpendicular vs. parallel to that of the STIRAP beams. We conclude that any polarization effects are small compared to our overall uncertainties.

## IV. THEORETICAL CALCULATION OF PI CROSS SECTIONS

The photoionization of alkali-metals has enjoyed considerable theoretical attention. Hartree-Fock, valence-electron potential and many-body perturbation theories have been applied to the photoionization of the ground and excited state atoms with various degrees of success [11,16,26–28]. Of these distinctly different techniques, the valence-electron model potential method has seen the widest application to the photoionization of excited atoms.

Our calculations of excited-state photoionization of the rubidium atom are performed in the central field approximation, where the motion of the valence electron is considered in the presence of a frozen core in a model-potential representation. The nonlinear parameters of the one active-electron potential have been variationally adjusted to reproduce measured valence energy levels, and several other observables such as static dipole polarizabilities [29]. The parametric model potential has the form

$$V_{\ell}(r) = \frac{Z_{\ell}(r)}{r} - \frac{\alpha_d}{2r^4}[1 - e^{(-r/r_c^{(\ell)})^6}], \tag{4}$$

where $\alpha_d$ is the static dipole polarizability of the $Rb^+$ ionic core and $Z_{\ell}(r)$ is an effective radial charge. The angular momentum-dependent parameters

$$Z_{\ell}(r) = 1 + (z-1)e^{-a_1(\ell)r} + r(a_3^{(\ell)} + a_4^{(\ell)}r)e^{-a_2^{(\ell)}r} \tag{5}$$

and the cutoff radius $r_c^{(\ell)}$ are obtained through a nonlinear fit to one-electron Rydberg energy levels. The cutoff radius is introduced to truncate the extent of the polarization potential near the nucleus, where it is unphysical. For Rb, the nuclear charge is $z = 37$.

The partial cross section in atomic units for the photoionization from a bound atomic state with $n\ell jmIF''M''$ quantum numbers is

$$\sigma_{n\ell j}(\omega) = \frac{4\pi^2\omega}{137(2F''+1)} \times \sum_{F_f M''} |\langle \epsilon\ell' j' m' I F_f M'' | r_q^{(1)} | n\ell j I F'' M'' \rangle|^2, \tag{6}$$

where $r_q^{(1)}$ is the first-rank irreducible dipole tensor and the symbols have their usual definition [30]. $F_f$ is the final value of the hyperfine angular momentum. The eigenstates $|\gamma\ell jIFM\rangle$ can be expanded over the fine-structure coupled states $|\gamma\ell jm\rangle$ as

$$|\gamma\ell jIFM\rangle=\sum_{m\mu}|\gamma\ell jm\rangle\langle jm,I\mu|FM\rangle. \tag{7}$$

The ensuing radial matrix elements have the form

$$\langle\epsilon\ell' j'm'|r_q^{(1)}|n\ell jm\rangle = (-1)^{\ell+1/2+j'+1}(2j'+1)^{1/2}\begin{Bmatrix}\ell & \ell' & 1\\ j' & j & 1/2\end{Bmatrix} \times\langle\epsilon\ell'\|\hat{r}^{(1)}\|n\ell\rangle\langle jm,1q|j'm'\rangle, \tag{8}$$

where the matrix element $\langle\epsilon\ell'\|\hat{r}^{(1)}\|n\ell\rangle$ is the reduced radial matrix element, connecting the initial state to the final energy-normalized state $|\epsilon\ell'\rangle$ at the photoelectron energy $\epsilon$. The dipole tensor $\hat{r}^{(1)}$ is dressed in the presence of the core electrons as

$$\hat{r}^{(1)}=r^{(1)}\left(1-\frac{\alpha_d}{r^3}\right). \tag{9}$$

Under the current experimental conditions, the initial state is defined as $|n\ell jIF''M''\rangle=|5D\tfrac{5}{2}\tfrac{5}{2}5M''\rangle$ with an equal population of the $5D_{5/2}$,$F''=5$,$M''$ sublevels, i.e., $M''=-3$ to $+3$. This is consistent with equally populated ground state ($5S_{1/2}$,$F=3$) magnetic sublevels: $M=-3$ to $+3$ (as expected in a MOT) which are then excited with linearly polarized STIRAP beams. As discussed in Sec. III, we see no significant dependence on the various polarizations. The calculated photoionization cross section as a function of photoelectron energy is shown in Fig. 8. The agreement between experiment and theory is well within the uncertainties. Total photoionization of Rb(5D) at threshold has been calculated by Aymar *et al.* [27] to be ~45 Mb; see Fig. 6 in Ref. [27]. When an average over initial states ($m_F$, $F$, $J$) is performed, our calculated cross section at threshold is $\sigma_{5D}(\epsilon=0)=44.3$ Mb. Aymar *et al.* also calculated the threshold cross section for PI of Rb(4D) level to be 34.0 Mb; see Table 1 (iii) in Ref. [27]. Our value for the PI of the same level at threshold is 33.9 Mb. As an additional check, we calculate the cross sections for photoionization from the Rb($5P_{3/2}$) level at 413 and 407 nm, $\sigma_{5P_{3/2}}=12.2$ and $\sigma_{5P_{3/2}}=11.9$ Mb, respectively. These cross sections have been previously measured via MOT trap loss to be 13.6(1.2) and 12.5(1.1) Mb, respectively [2].

## V. SUMMARY

In conclusion, we have used a combination of efficient population transfer and a trap loss technique to investigate photoionization (PI) of the Rb($5D_{5/2}$) level. Pulses in the counterintuitive order are used to drive a two-photon transition to the $5D_{5/2}$ level. The PI rate from this level is measured by the rate at which atoms leave the trap. We measure not only the absolute value but also the wavelength dependence of the PI cross section using both cw and pulsed ionizing radiation. We also calculate the PI cross section as a function of wavelength and obtain good agreement with our measurements. This technique can obviously be extended to measure photoionization from other states and in other atoms. Once the cross sections are known, the trap loss can then serve to calibrate excitation efficiency. This work is another example of the power of using trap loss to measure the absolute cross section for an atomic process.

## ACKNOWLEDGMENTS

We thank Wenko Süptitz and Jared Bartholomew for early contributions to this work and Paul Lett and John Weiner for the loan of the Nd:YAG laser. This work was supported in part by the Division of Chemical Sciences, Office of Basic Energy Sciences, Office of Energy Research, U.S. Department of Energy. V.S.-V. gratefully acknowledges the support of CONACyT (Grant No. 28511-E), the United States–Mexico Foundation for Science and the Mexican Academy of Sciences.

[1] H.J. Metcalf and P. van der Straten, *Laser Cooling and Trapping* (Springer, New York, 1999).
[2] T.P. Dinneen, C.D. Wallace, K.Y.N. Tan, and P.L. Gould, Opt. Lett. **17**, 1706 (1992).
[3] C. Gabbanini, S. Gozzini, and A. Lucchesini, Opt. Commun. **141**, 25 (1997).
[4] O. Marago, D. Ciampini, F. Fuso, E. Arimondo, C. Gabbanini, and S.T. Manson, Phys. Rev. A **57**, R4110 (1998).
[5] B.M. Patterson, T. Takekoshi, and R.J. Knize, Phys. Rev. A **59**, 2508 (1999).
[6] F. Ruschewitz, J. L. Peng, R. Degner, H. Hinderthuer, D. Scheller, D. Bettermann, W. Ertmer, in *Proceedings of the 1996 European Quantum Electronics Conference*, p. 112.
[7] K. Sengstock and W. Ertmer, (private communication).
[8] R.S. Schappe, P. Feng, L.W. Anderson, C.C. Lin, and T. Walker, Europhys. Lett. **29**, 439 (1995).
[9] R.S. Schappe, T. Walker, L.W. Anderson, and C.C. Lin, Phys. Rev. Lett. **76**, 4328 (1996).
[10] F.J. Wuilleumier, D.L. Ederer, and J.L. Picque, Adv. At., Mol., Opt. Phys. **23**, 197 (1988).
[11] D. Petrov, V.L. Sukhorukov, E. Leber, and H. Hotop, Eur. Phys. J. D **10**, 53 (2000).
[12] A.V. Smith, J.E.M. Goldsmith, D.E. Nitz, and S.J. Smith, Phys. Rev. A **22**, 577 (1980).
[13] K. Gerwert and K.J. Kollath, J. Phys. B **16**, L217 (1983).
[14] K.D. Bonin, M. Gatzke, C.L. Collins, and M.A. Kadar-Kallen, Phys. Rev. A **39**, 5624 (1989).
[15] D.J. Armstrong, L.A. Westling, and S.J. Smith, Phys. Rev. A **43**, 6398 (1991).
[16] J. Lahiri and S.T. Manson, Phys. Rev. A **33**, 3151 (1986).
[17] C. Monroe, W. Swann, H. Robinson, and C. Wieman, Phys. Rev. Lett. **65**, 1571 (1990).
[18] L. Ricci, M. Weidemüller, T. Esslinger, A. Hemmerich, C. Zimmerman, V. Vuletic, W. Köneg, and T.W. Hänsch, Opt. Commun. **117**, 541 (1995).

[19] W. Süptitz, B.C. Duncan, and P.L. Gould, J. Opt. Soc. Am. B **14**, 1001 (1997).
[20] K. Bergmann, H. Theuer, and B.W. Shore, Rev. Mod. Phys. **70**, 1003 (1998).
[21] T.P. Dinneen, C.D. Wallace, and P.L. Gould, Opt. Commun. **92**, 277 (1992).
[22] T.T. Grove, V. Sanchez-Villicana, B.C. Duncan, S. Maleki, and P.L. Gould, Phys. Scr. **52**, 271 (1995).
[23] O.S. Heavens, J. Opt. Soc. Am. **51**, 1058 (1961).
[24] D. Hoffmann, P. Feng, R.S. Williamson III, and T. Walker, Phys. Rev. Lett. **69**, 753 (1992).
[25] F. Fuso, D. Ciampini, E. Arimondo, and C. Gabbanini, Opt. Commun. **173**, 223 (2000).
[26] D.W. Norcross, Phys. Rev. A **7**, 606 (1976).
[27] M. Aymar, O. Robaux, and S. Wane, J. Phys. B **17**, 993 (1984).
[28] A. Derevianko, W.R. Johnson, and H.R. Sadeghpour, Phys. Rev. A **61**, 022506 (2000).
[29] M. Marinescu, H.R. Sadeghpour, and A. Dalgarno, Phys. Rev. A **49**, 982 (1994).
[30] I.I. Sobelman, *Atomic Spectra and Radiative Transitions*, Springer Series in Chemical Physics 1 (Springer Verlag, Berlin, 1978).